

Gluon polarization in the nucleon from quasi-real photoproduction of high- p_T hadron pairs

The COMPASS Collaboration

Abstract

We present a determination of the gluon polarization $\Delta G/G$ in the nucleon, based on the helicity asymmetry of quasi-real photoproduction events, $Q^2 < 1 \text{ (GeV}/c)^2$, with a pair of large transverse-momentum hadrons in the final state. The data were obtained by the COMPASS experiment at CERN using a 160 GeV polarized muon beam scattered on a polarized ^6LiD target. The helicity asymmetry for the selected events is $\langle A_{\parallel}/D \rangle = 0.002 \pm 0.019(\text{stat.}) \pm 0.003(\text{syst.})$. From this value, we obtain in a leading-order QCD analysis $\Delta G/G = 0.024 \pm 0.089(\text{stat.}) \pm 0.057(\text{syst.})$ at $x_g = 0.095$ and $\mu^2 \simeq 3 \text{ (GeV}/c)^2$.

(Submitted to Physics Letters B)

E.S. Ageev²⁴⁾, V.Yu. Alexakhin⁸⁾, Yu. Alexandrov¹⁸⁾, G.D. Alexeev⁸⁾, A. Amoroso²⁹⁾,
 B. Badelek³⁰⁾, F. Balestra²⁹⁾, J. Ball²⁵⁾, G. Baum¹⁾, Y. Bedfer²⁵⁾, P. Berglund¹³⁾,
 C. Bernet^{11,25)}, R. Bertini²⁹⁾, R. Birsas²⁸⁾, J. Bisplinghoff³⁾, P. Bordalo^{15,a)},
 F. Bradamante²⁸⁾, A. Bravar¹⁶⁾, A. Bressan²⁸⁾, G. Brona³⁰⁾, E. Burtin²⁵⁾, M.P. Bussa²⁹⁾,
 V.N. Bytchkov⁸⁾, L. Cerini²⁸⁾, A. Chapiro²⁷⁾, A. Cicuttin²⁷⁾, M. Colantoni^{29,b)},
 A.A. Colavita²⁷⁾, S. Costa²⁹⁾, M.L. Crespo²⁷⁾, S. Dalla Torre²⁸⁾, S.S. Dasgupta⁶⁾,
 N. Dedek¹⁹⁾, R. De Masi²⁰⁾, O.Yu. Denisov^{29,c)}, L. Dhara⁷⁾, V. Diaz²⁷⁾,
 A.M. Dinkelbach²⁰⁾, A.V. Dolgoplov²⁴⁾, S.V. Donskov²⁴⁾, V.A. Dorofeev²⁴⁾,
 N. Doshita^{21,2)}, V. Duic²⁸⁾, W. Dünneberger¹⁹⁾, J. Ehlers^{12,16)}, P.D. Eversheim³⁾,
 W. Eylich⁹⁾, M. Fabro²⁸⁾, M. Faessler¹⁹⁾, V. Falaleev¹¹⁾, P. Fauland¹⁾, A. Ferrero²⁹⁾,
 L. Ferrero²⁹⁾, M. Finger²²⁾, M. Finger jr.⁸⁾, H. Fischer¹⁰⁾, J. Franz¹⁰⁾, J.M. Friedrich²⁰⁾,
 V. Frolov^{29,c)}, R. Garfagnini²⁹⁾, F. Gautheron¹⁾, O.P. Gavrichtchouk⁸⁾,
 S. Gerassimov^{18,20)}, R. Geyer¹⁹⁾, M. Giorgi²⁸⁾, B. Gobbo²⁸⁾, S. Goertz^{2,4)}, A.M. Gorin²⁴⁾,
 O.A. Grajek³⁰⁾, A. Grasso²⁹⁾, B. Grube²⁰⁾, A. Grünemaier¹⁰⁾, J. Hannappel⁴⁾, D. von
 Harrach¹⁶⁾, T. Hasegawa¹⁷⁾, S. Hedicke¹⁰⁾, F.H. Heinsius^{10,11)}, R. Hermann¹⁶⁾, C. Heß²⁾,
 F. Hinterberger³⁾, M. von Hodenberg¹⁰⁾, N. Horikawa²¹⁾, S. Horikawa^{21,11)}, N. d'Hose²⁵⁾,
 R.B. Ijaduola²⁷⁾, C. Ilgner¹⁹⁾, A.I. Ioukaev⁸⁾, S. Ishimoto²¹⁾, O. Ivanov⁸⁾, T. Iwata²¹⁾,
 R. Jahn³⁾, A. Janata⁸⁾, R. Joosten³⁾, N.I. Jouravlev⁸⁾, E. Kabuß¹⁶⁾, V. Kalinnikov²⁸⁾,
 D. Kang¹⁰⁾, F. Karstens¹⁰⁾, W. Kastaun¹⁰⁾, B. Ketzer²⁰⁾, G.V. Khaustov²⁴⁾,
 Yu.A. Khokhlov²⁴⁾, N.V. Khomutov⁸⁾, Yu. Kisselev^{1,2)}, F. Klein⁴⁾, S. Koblitiz¹⁶⁾,
 J.H. Koivuniemi^{13,2)}, V.N. Kolosov²⁴⁾, E.V. Komissarov⁸⁾, K. Kondo^{21,2)},
 K. Königsmann¹⁰⁾, A.K. Konoplyannikov²⁴⁾, I. Konorov^{18,20)}, V.F. Konstantinov²⁴⁾,
 A.S. Korentchenko⁸⁾, A. Korzenev^{16,c)}, A.M. Kotzinian^{8,29)}, N.A. Koutchinski⁸⁾,
 K. Kowalik³⁰⁾, N.P. Kravchuk⁸⁾, G.V. Krivokhizhin⁸⁾, Z.V. Kroumchtein⁸⁾, R. Kuhn²⁰⁾,
 F. Kunne²⁵⁾, K. Kurek³⁰⁾, M.E. Ladygin²⁴⁾, M. Lamanna^{11,28)}, M. Leberig^{11,16)}, J.M. Le
 Goff²⁵⁾, J. Lichtenstadt²⁶⁾, T. Liska²³⁾, I. Ludwig¹⁰⁾, A. Maggiora²⁹⁾, M. Maggiora²⁹⁾,
 A. Magnon²⁵⁾, G.K. Mallot¹¹⁾, I.V. Manuilov²⁴⁾, C. Marchand²⁵⁾, J. Marroncle²⁵⁾,
 A. Martin²⁸⁾, J. Marzec³¹⁾, T. Matsuda¹⁷⁾, A.N. Maximov⁸⁾, K.S. Medved⁸⁾, W. Meyer²⁾,
 A. Mielech^{28,30)}, Yu.V. Mikhailov²⁴⁾, M.A. Moinester²⁶⁾, O. Nähle³⁾, J. Nassalski³⁰⁾,
 S. Neliba²³⁾, D.P. Neyret²⁵⁾, V.I. Nikolaenko²⁴⁾, A.A. Nozdrin⁸⁾, V.F. Obraztsov²⁴⁾,
 A.G. Olshevsky⁸⁾, M. Ostrick⁴⁾, A. Padee³¹⁾, P. Pagano²⁸⁾, S. Panebianco²⁵⁾,
 D. Panzieri^{29,b)}, S. Paul²⁰⁾, H.D. Pereira^{10,25)}, D.V. Peshekhonov⁸⁾, V.D. Peshekhonov⁸⁾,
 G. Piragino²⁹⁾, S. Platchkov²⁵⁾, K. Platzer¹⁹⁾, J. Pochodzalla¹⁶⁾, V.A. Polyakov²⁴⁾,
 A.A. Popov⁸⁾, J. Pretz^{4,11)}, S. Procureur²⁵⁾, C. Quintans¹⁵⁾, S. Ramos^{15,a)},
 P.C. Rebougeard²⁵⁾, G. Reicherz²⁾, J. Reymann¹⁰⁾, K. Rith^{9,11)}, E. Rondio³⁰⁾,
 A.M. Rozhdestvensky⁸⁾, A.B. Sadovski⁸⁾, E. Saller⁸⁾, V.D. Samoylenko²⁴⁾, A. Sandacz³⁰⁾,
 M. Sans¹⁹⁾, M.G. Sapozhnikov⁸⁾, I.A. Savin⁸⁾, P. Schiavon²⁸⁾, C. Schill¹⁰⁾, T. Schmidt¹⁰⁾,
 H. Schmitt¹⁰⁾, L. Schmitt^{20,m)}, O.Yu. Shevchenko⁸⁾, A.A. Shishkin⁸⁾, H.-W. Siebert¹²⁾,
 L. Sinha⁷⁾, A.N. Sissakian⁸⁾, A. Skachkova²⁹⁾, M. Slunicka⁸⁾, G.I. Smirnov⁸⁾, F. Sozzi²⁸⁾,
 A. Srnka⁵⁾, F. Stinzing⁹⁾, M. Stolarski³⁰⁾, V.P. Sugonyaev²⁴⁾, M. Sulc¹⁴⁾, R. Sulej³¹⁾,
 N. Takabayashi²¹⁾, V.V. Tchalishvili⁸⁾, F. Tessarotto²⁸⁾, A. Teufel⁹⁾, D. Thers²⁵⁾,
 L.G. Tkatchev⁸⁾, T. Toeda²¹⁾, V.I. Tretyak⁸⁾, S. Trousov⁸⁾, M. Varanda¹⁵⁾, M. Virius²³⁾,
 N.V. Vlassov⁸⁾, M. Wagner⁹⁾, R. Webb⁹⁾, E. Weise³⁾, Q. Weitzel²⁰⁾, U. Wiedner¹⁹⁾,
 M. Wiesmann²⁰⁾, R. Windmolders⁴⁾, S. Wirth⁹⁾, W. Wiślicki³⁰⁾, A.M. Zanetti²⁸⁾,
 K. Zaremba³¹⁾, J. Zhao¹⁶⁾, R. Ziegler³⁾, and A. Zvyagin¹⁹⁾

-
- ¹⁾ Universität Bielefeld, Fakultät für Physik, 33501 Bielefeld, Germany^{d)}
 - ²⁾ Universität Bochum, Institut für Experimentalphysik, 44780 Bochum, Germany^{d)}
 - ³⁾ Universität Bonn, Helmholtz-Institut für Strahlen- und Kernphysik, 53115 Bonn, Germany^{d)}
 - ⁴⁾ Universität Bonn, Physikalisches Institut, 53115 Bonn, Germany^{d)}
 - ⁵⁾ Institute of Scientific Instruments, AS CR, 61264 Brno, Czech Republic^{e)}
 - ⁶⁾ Burdwan University, Burdwan 713104, India^{g)}
 - ⁷⁾ Matrivani Institute of Experimental Research & Education, Calcutta-700 030, India^{h)}
 - ⁸⁾ Joint Institute for Nuclear Research, 141980 Dubna, Moscow region, Russia
 - ⁹⁾ Universität Erlangen–Nürnberg, Physikalisches Institut, 91054 Erlangen, Germany^{d)}
 - ¹⁰⁾ Universität Freiburg, Physikalisches Institut, 79104 Freiburg, Germany^{d)}
 - ¹¹⁾ CERN, 1211 Geneva 23, Switzerland
 - ¹²⁾ Universität Heidelberg, Physikalisches Institut, 69120 Heidelberg, Germany^{d)}
 - ¹³⁾ Helsinki University of Technology, Low Temperature Laboratory, 02015 HUT, Finland and University of Helsinki, Helsinki Institute of Physics, 00014 Helsinki, Finland
 - ¹⁴⁾ Technical University in Liberec, 46117 Liberec, Czech Republic^{e)}
 - ¹⁵⁾ LIP, 1000-149 Lisbon, Portugal^{f)}
 - ¹⁶⁾ Universität Mainz, Institut für Kernphysik, 55099 Mainz, Germany^{d)}
 - ¹⁷⁾ University of Miyazaki, Miyazaki 889-2192, Japanⁱ⁾
 - ¹⁸⁾ Lebedev Physical Institute, 119991 Moscow, Russia
 - ¹⁹⁾ Ludwig-Maximilians-Universität München, Department für Physik, 80799 Munich, Germany^{d)}
 - ²⁰⁾ Technische Universität München, Physik Department, 85748 Garching, Germany^{d)}
 - ²¹⁾ Nagoya University, 464 Nagoya, Japanⁱ⁾
 - ²²⁾ Charles University, Faculty of Mathematics and Physics, 18000 Prague, Czech Republic^{e)}
 - ²³⁾ Czech Technical University in Prague, 16636 Prague, Czech Republic^{e)}
 - ²⁴⁾ State Research Center of the Russian Federation, Institute for High Energy Physics, 142281 Protvino, Russia
 - ²⁵⁾ CEA DAPNIA/SPhN Saclay, 91191 Gif-sur-Yvette, France
 - ²⁶⁾ Tel Aviv University, School of Physics and Astronomy, 69978 Tel Aviv, Israel^{j)}
 - ²⁷⁾ ICTP–INFN MLab Laboratory, 34014 Trieste, Italy
 - ²⁸⁾ INFN Trieste and University of Trieste, Department of Physics, 34127 Trieste, Italy
 - ²⁹⁾ INFN Turin and University of Turin, Physics Department, 10125 Turin, Italy
 - ³⁰⁾ Soltan Institute for Nuclear Studies and Warsaw University, 00-681 Warsaw, Poland^{k)}
 - ³¹⁾ Warsaw University of Technology, Institute of Radioelectronics, 00-665 Warsaw, Poland^{l)}
 - ^{a)} Also at IST, Universidade Técnica de Lisboa, Lisbon, Portugal
 - ^{b)} Also at University of East Piedmont, 15100 Alessandria, Italy
 - ^{c)} On leave of absence from JINR Dubna
 - ^{d)} Supported by the German Bundesministerium für Bildung und Forschung
 - ^{e)} Supported by Czech Republic MEYS grants ME492 and LA242
 - ^{f)} Supported by the Portuguese FCT - Fundação para a Ciência e Tecnologia grants POCTI/FNU/49501/2002 and POCTI/FNU/50192/2003
 - ^{g)} Supported by UGC-DSA II grants, Govt. of India
 - ^{h)} Supported by the Shailabala Biswas Education Trust
 - ⁱ⁾ Supported by the Ministry of Education, Culture, Sports, Science and Technology, Japan
 - ^{j)} Supported by the Israel Science Foundation, funded by the Israel Academy of Sciences and Humanities
 - ^{k)} Supported by KBN grant nr 621/E-78/SPUB-M/CERN/P-03/DZ 298 2000 and nr 621/E-78/SPB/CERN/P-03/DWM 576/2003-2006, and the MNII research funds for 2005-2007
 - ^{l)} Supported by KBN grant nr 134/E-365/SPUB-M/CERN/P-03/DZ299/2000
 - ^{m)} Also at Gesellschaft für Schwerionenforschung, Darmstadt, Germany

1 Introduction

The decomposition of the nucleon spin in terms of the contributions from its constituents has been a central topic in polarized deep-inelastic scattering (DIS) for the last twenty years. The European Muon Collaboration study of the proton spin structure [1] has shown that the spin of the quarks only contributes to a small fraction $\Delta\Sigma$ of the proton spin. This result has been confirmed by several experiments on the proton, the deuteron, and ^3He , establishing $\Delta\Sigma$ between 20% and 30% [2, 3], in contrast to the 60% expected in the quark-parton model [4].

Another contribution to the nucleon spin, ΔG , originates from the spin of the gluons. In inclusive DIS, it can only be determined from the Q^2 dependence of the spin structure function g_1 . Next-to-Leading Order (NLO) QCD analyses provide estimates for ΔG below or around unity at a scale of 3 (GeV/c) 2 . The precision of these fits is however strongly limited by the small Q^2 range covered by the data.

In semi-inclusive DIS or in proton–proton scattering, the final state can be used to select hard processes involving gluons from the nucleon. In polarized semi-inclusive DIS, the polarization $\Delta G/G$ of gluons carrying a fraction x_g of the nucleon momentum is obtained from the cross-section helicity asymmetry of the photon–gluon fusion (PGF), $\gamma^* g \rightarrow q\bar{q}$.

Two procedures have been proposed to tag this process. The first one consists in selecting open-charm events, which provides the purest sample of PGF events [5, 6], but at a low rate. Another possibility is to select events with two jets at high transverse momentum, p_T , with respect to the virtual photon direction or, in fixed-target experiments, two high- p_T hadrons [7]. The latter procedure provides much larger statistics but leaves a significant fraction of background events in the selected sample. As a result, the cross-section helicity asymmetry A_{\parallel} contains in addition to the contribution from PGF a contribution A_{bgd} from the background processes:

$$A_{\parallel} = R_{\text{PGF}} \hat{a}_{\text{LL}}^{\text{PGF}} \frac{\Delta G}{G} + A_{\text{bgd}}. \quad (1)$$

Here, R_{PGF} is the fraction of PGF events and $\hat{a}_{\text{LL}}^{\text{PGF}} \equiv d\Delta\sigma_{\text{PGF}}^{\mu g}/d\sigma_{\text{PGF}}^{\mu g}$ is the analyzing power of PGF that is the helicity asymmetry of the hard lepton–gluon scattering cross-section. This quantity is calculated from the leading order expressions of the polarized and unpolarized partonic cross-sections. On the other hand, R_{PGF} and A_{bgd} must be estimated by a simulation, which introduces a model dependence in the evaluation of $\Delta G/G$.

This paper presents a measurement of the cross-section helicity asymmetry obtained for the large sample of muon–deuteron events collected by the COMPASS experiment at CERN in the low virtuality domain, $Q^2 < 1$ (GeV/c) 2 . We select interactions in which a pair of high- p_T hadrons is produced. The gluon polarization $\Delta G/G$ is extracted from this asymmetry using the event generator PYTHIA 6.2 [8] and leading-order expressions for the analyzing powers of the PGF and of the background processes. Possible spin effects in the fragmentation are neglected.

2 Experimental set-up

The experiment [9] is located at the M2 beam line of the CERN SPS, which provides a 160 GeV μ^+ beam at a rate of 2×10^8 muons per spill of 4.8 s with a cycle time of 16.8 s. The muons are produced in the decay of pions and kaons, and the beam has a natural polarization of $\langle P_b \rangle = -0.76$, with a relative accuracy of 5% [10]. The incident muon momentum is measured upstream of the experimental area in a beam spectrometer,

while its direction and position at the entrance of the target are determined in a telescope of scintillating fiber hodoscopes and silicon microstrip detectors.

The polarized target system [11] consists of an upstream cell (u) and a downstream cell (d), each 60 cm long and 3 cm in diameter, separated by 10 cm. The cells are located on the axis of a superconducting solenoid magnet providing a field of 2.5 T along the beam direction, and are filled with ^6LiD . This material is used as a deuteron target and was selected for its high dilution factor f of about 40%, which accounts for the fact that only a fraction of the target nucleons are polarizable. Typical polarization values of 50% are obtained by dynamic nuclear polarization, and measured with a relative accuracy of 5%. The two cells are polarized in opposite directions by using different microwave frequencies so that data with both spin orientations are recorded simultaneously. The muon flux then cancels out in the counting rate asymmetry. However, the acceptance of the spectrometer is not identical for the two cells, which gives rise to an acceptance asymmetry. To account for this, a rotation of the magnetic field is performed in order to reverse the orientation of the spins in each cell. The acceptance asymmetry then disappears in the sum between the counting rate asymmetries before and after rotation (for details, see Eq. 2). A perfect cancellation requires the ratio $L_u a_u / L_d a_d$ to be the same before and after rotation, where L_u, L_d are the luminosities and a_u, a_d the acceptances for the upstream and downstream target cells. False asymmetries due to the variations of this ratio with time are minimized by performing the rotation frequently, i.e. every 8 hours. However, because of the change in the orientation of the target field, the set-up is slightly different before and after rotation, which affects the $L_u a_u / L_d a_d$ ratio. To cancel this effect the orientation of the spins for a given field orientation is reversed by repolarization a few times during the running period.

The COMPASS spectrometer has a large angle and a small angle spectrometer built around two dipole magnets, in order to allow the reconstruction of the scattered muon and of the produced hadrons in broad momentum and angular ranges. Different types of tracking detectors are used to deal with the rapid variation of the particle flux density with the distance from the beam. Tracking in the beam region is performed by scintillating fibers. Up to 20 cm from the beam we use Micromegas and GEMs. Further away, tracking is carried out in multiwire proportional chambers and drift chambers. Large-area trackers, based on straw detectors and large drift chambers extend the tracking over a surface of up to several square meters. Muons are identified by dedicated trackers placed downstream of hadron absorbers. Hadron/muon separation is strengthened by two large iron-scintillator sampling calorimeters, installed upstream of the hadron absorbers and shielded to avoid electromagnetic contamination. The particle identification provided by the ring imaging Cherenkov detector is not used in the present analysis.

The trigger system [12] provides efficient tagging down to $Q^2 = 0.002 \text{ (GeV}/c)^2$, by detecting the scattered muon in a set of hodoscopes placed behind the two dipole magnets. A large enough energy deposit in the hadronic calorimeters is required in order to suppress unwanted triggers generated by halo muons, elastic muon-electron scattering events, and radiative events.

3 Asymmetry measurement

The present analysis deals with data collected in 2002 and 2003. The selected events are required to contain at least two charged hadrons associated to the primary vertex, in addition to the incident and scattered muons. We consider events with $0.35 < y < 0.9$, where y is the fraction of energy lost by the incident muon. The lower y cut removes events with a low sensitivity to the gluon polarization, while the upper one rejects events which

could be affected by large radiative effects. Since PYTHIA provides a reliable model for interactions of virtual photons with nucleons at low virtuality [13], we select events with $Q^2 < 1 \text{ (GeV/c)}^2$, which corresponds to about 90% of the total data set. The DIS sample, $Q^2 > 1 \text{ (GeV/c)}^2$, is being analyzed separately using LEPTO which is better adapted to this domain.

Furthermore, cuts are applied on the two hadrons with highest transverse momentum. The muon contamination of the hadron sample is eliminated by requiring the energy deposit in the calorimeters to be large enough with respect to the reconstructed momentum, $E/p > 0.3$. In addition, hadron candidates detected also downstream of the hadron absorbers are discarded. The invariant mass of the two-hadron system is required to be larger than $1.5 \text{ GeV}/c^2$, and x_F to be larger than 0.1, where $x_F = 2p_L^*/W$. Here, p_L^* is the longitudinal momentum of the hadron in the photon–nucleon center of mass frame and W is the invariant mass of the hadronic final state. Finally, the fraction of PGF events in the sample is enhanced by requiring the transverse momentum of the two hadrons to be large: $p_T^{h1} > 0.7 \text{ GeV}/c$, $p_T^{h2} > 0.7 \text{ GeV}/c$ and $(p_T^{h1})^2 + (p_T^{h2})^2 > 2.5 \text{ (GeV/c)}^2$, as in the SMC high- p_T analysis [14]. In total, around 250 000 events remain after these cuts, defining the high- p_T sample.

The asymmetry A_{\parallel} can be obtained from the number of events in the upstream and downstream cells, before and after field rotation:

$$A_{\parallel} = \frac{1}{2|P_b P_t f|} \left(\frac{N_u^{\uparrow\downarrow} - N_d^{\uparrow\uparrow}}{N_u^{\uparrow\downarrow} + N_d^{\uparrow\uparrow}} + \frac{N_d^{\uparrow\downarrow} - N_u^{\uparrow\uparrow}}{N_d^{\uparrow\downarrow} + N_u^{\uparrow\uparrow}} \right). \quad (2)$$

The two terms in this expression correspond to opposite orientations of the target magnetic field, with for example $N_u^{\uparrow\downarrow}$ the number of events in the upstream cell when the cell polarization is anti-parallel to the beam polarization.

The statistical error on the asymmetry is minimized by weighting each event with its overall sensitivity to the gluon polarization [15]. The event weight is taken to be $w = fDP_b$, where D is a kinematic factor which approximates the amount of polarization transferred from the incident muon to the virtual photon:

$$D = \frac{y(2 - y - \frac{2m^2 y^2}{Q^2(1-xy)})}{(1 + (1 - y)^2 - \frac{2m^2 y^2}{Q^2}) \sqrt{1 - \frac{4m^2(1-x)xy^2}{Q^2(1-xy)^2}}}. \quad (3)$$

Here, all terms containing the muon mass m were taken into account since the sample of events is at low Q^2 . The factor D is proportional to the analyzing power of PGF apart from a weak dependence on the event kinematics, and was therefore used in the weight instead of $\hat{a}_{LL}^{\text{PGF}}$ which is unknown on an event-by-event basis. The average value of D is around 0.6. In the weighting method, the expression for the asymmetry becomes

$$\left\langle \frac{A_{\parallel}}{D} \right\rangle = \frac{1}{2|P_t|} \left(\frac{\Sigma w_u^{\uparrow\downarrow} - \Sigma w_d^{\uparrow\uparrow}}{\Sigma (w_u^{\uparrow\downarrow})^2 + \Sigma (w_d^{\uparrow\uparrow})^2} + \frac{\Sigma w_d^{\uparrow\downarrow} - \Sigma w_u^{\uparrow\uparrow}}{\Sigma (w_d^{\uparrow\downarrow})^2 + \Sigma (w_u^{\uparrow\uparrow})^2} \right). \quad (4)$$

With the high- p_T sample defined above, we obtain

$$\left\langle \frac{A_{\parallel}}{D} \right\rangle = 0.002 \pm 0.019(\text{stat}) \pm 0.003(\text{syst}). \quad (5)$$

The systematic error accounts for the false asymmetries, which were estimated using a sample of low p_T events with much larger statistics. Other sources of systematic errors,

including the error on the beam and target polarizations, are proportional to the (small) measured asymmetry, and have been neglected.

4 Gluon polarization

As stated before, the determination of the gluon polarization from the high- p_T asymmetry involves a Monte Carlo simulation. The generated events are propagated through a GEANT [16] model of the COMPASS spectrometer, and reconstructed using the same program as for real data. Finally, the same cuts as for real data are applied to obtain the Monte Carlo sample of high- p_T events.

We use PYTHIA to generate two different kinds of processes. In direct processes, for example the PGF, the virtual photon takes part directly in the hard partonic interaction. In resolved-photon processes, it fluctuates into a hadronic state from which a parton is extracted (the partonic structure of the virtual photon is resolved). This parton then interacts with a parton from the nucleon. At $Q^2 < 1 \text{ (GeV/c)}^2$, the resolved-photon processes constitute about half of the high- p_T sample. For $Q^2 > 1 \text{ (GeV/c)}^2$, their contribution drops to about 10%, and it becomes negligible for $Q^2 > 2 \text{ (GeV/c)}^2$. To compute the asymmetry of a given process, it is mandatory to find a hard scale μ^2 allowing the factorization of the cross-sections into a hard partonic cross-section calculable perturbatively, and a soft parton distribution function which needs to be measured. In Eq. (1) for instance, the asymmetry of the PGF factorizes into a hard asymmetry (the analyzing power) and a soft asymmetry (the gluon polarization). In our case, Q^2 is too small to be used as a scale. However, the scale provided by PYTHIA¹⁾ is very close to the p_T^2 of one of the partons produced in the hard reaction. Since the p_T cut applied to the two highest- p_T hadrons implies, for most of the events, large transverse momentum partons in the final state of the hard reaction, this quantity turns out to be large enough. Events for which no hard scale can be found are classified in PYTHIA as “low- p_T processes.”

After varying many parameters of PYTHIA, the best agreement with our data was obtained by modifying only the width of the intrinsic transverse momentum distribution of partons within the resolved virtual photon²⁾, which was decreased from 1 GeV/c to 0.5 GeV/c.

The lower p_T cut-off³⁾ is set by default to 1 GeV/c to prevent the cross-section for $2 \rightarrow 2$ processes such as PGF from diverging when the partonic transverse momentum vanishes. However, this does not occur in our high- p_T sample, as the transverse-momentum distribution of the outgoing partons starts just below 1 GeV/c. To avoid cutting into this distribution, we have decreased the lower p_T cut-off to 0.9 GeV/c and did not observe any effect on the agreement with the data. The simulated and real data samples of high- p_T events are compared in Fig. 1 for Q^2 , y , and for the total and transverse momenta of the hadron with highest p_T . An equally good agreement is obtained for the second hadron.

Various processes contribute to the Monte Carlo sample of high- p_T events, as shown in Fig. 2. The direct processes are the PGF, the QCD Compton (QCDC, $\gamma^*q \rightarrow qg$), and the leading process ($\gamma^*q \rightarrow q$). For the resolved-photon processes, a parton f from the nucleon interacts with a parton f^γ from the virtual photon, where f and f^γ can be a quark or a gluon. We have neglected the resolved-photon processes $q\bar{q} \rightarrow q'\bar{q}'$, $q\bar{q} \rightarrow g\bar{g}$ and $g\bar{g} \rightarrow q\bar{q}$, which altogether represent only 0.6% of the sample. The low- p_T processes contain all events for which no hard scale can be found. Each of these processes contributes

¹⁾ Parameter MSTP(32).

²⁾ Parameter PARP(99) in Ref. [8].

³⁾ Parameter CKIN(5).

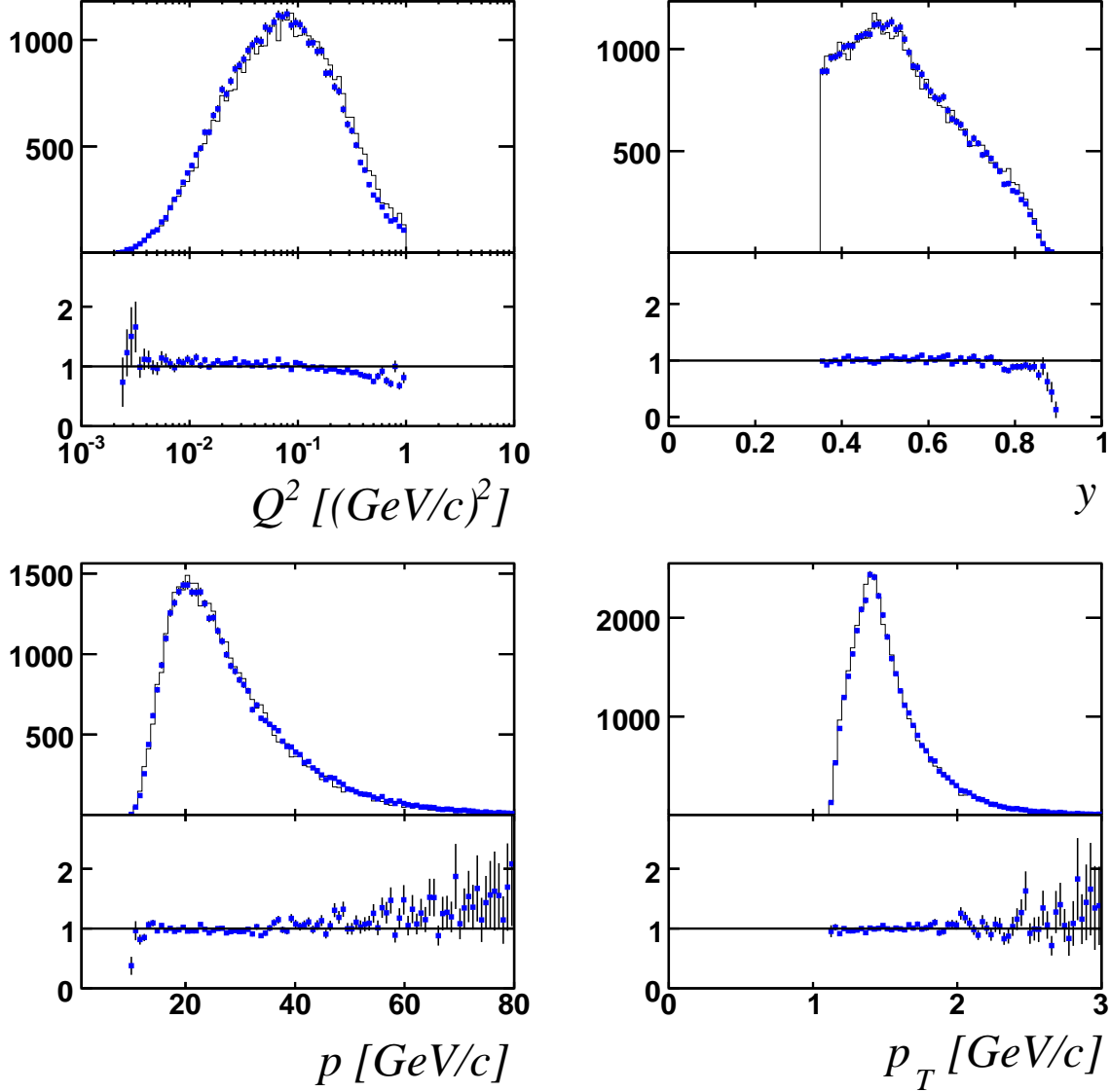


Figure 1: Comparison between data and Monte Carlo for Q^2 , y , and for the total (transverse) momentum p (p_T) of the hadron with highest p_T . The upper part of each plot shows the real data (points) and simulation (line), normalized to the same number of events. The lower part shows the corresponding data/Monte Carlo ratio.

to the cross-section helicity asymmetry, provided that a transverse photon is exchanged. The asymmetry can then be approximately expressed as

$$\begin{aligned}
\left\langle \frac{A_{\parallel}}{D} \right\rangle &= R_{\text{PGF}} \left\langle \frac{\hat{a}_{\text{LL}}^{\text{PGF}}}{D} \right\rangle \frac{\Delta G}{G} + R_{\text{QCDC}} \left\langle \frac{\hat{a}_{\text{LL}}^{\text{QCDC}}}{D} A_1 \right\rangle \\
&+ \sum_{f, f\gamma=u, d, s, \bar{u}, \bar{d}, \bar{s}, G} R_{ff\gamma} \left\langle \hat{a}_{\text{LL}}^{ff\gamma} \frac{\Delta f}{f} \frac{\Delta f\gamma}{f\gamma} \right\rangle \\
&+ R_{\text{leading}} \times A_{\text{leading}} + R_{\text{low-}p_T} \times A_{\text{low-}p_T}.
\end{aligned} \tag{6}$$

Here, R_{QCDC} is the fraction of QCD Compton events, and $R_{ff\gamma}$ is the fraction of events in the whole high- p_T sample for which a parton f from the nucleon interacts with a

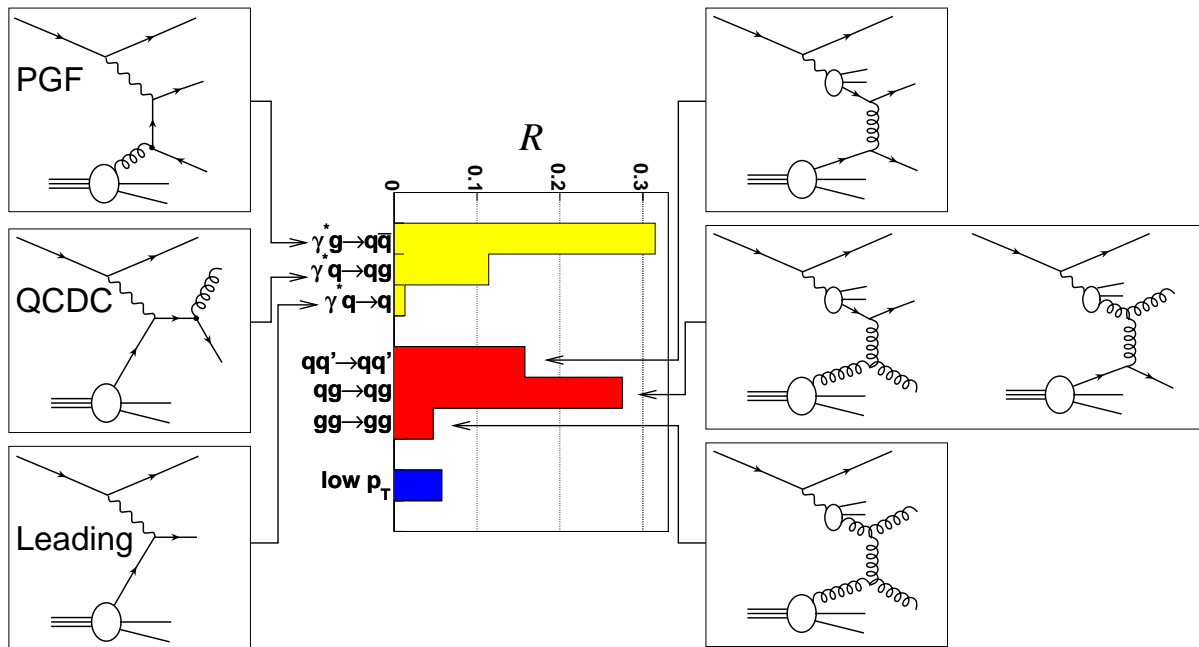


Figure 2: Relative contributions R of the dominant PYTHIA processes to the Monte Carlo sample of high- p_T events. Left: direct processes; right: resolved-photon processes.

parton f^γ from a resolved photon. Recalling that we use a deuteron target, A_1 is the inclusive virtual-photon–deuteron asymmetry and $\Delta f/f$ ($\Delta f^\gamma/f^\gamma$) is the polarization of quarks or gluons in the deuteron (photon). The contributions of the leading and low- p_T processes cannot be calculated in the same way, since there is no hard scale allowing the factorization of their asymmetries A_{leading} and $A_{\text{low-}p_T}$ (low transverse momentum, and $Q^2 < 1$ (GeV/c) 2 events). However, the asymmetry for this kind of events is small as indicated by previous measurements of A_1 at low Q^2 [17]. Moreover, the leading and low- p_T processes together account for only 7% of the high- p_T sample. For these two reasons, we neglected their contributions.

The fraction of photon–gluon fusion events in the sample is of the order of 30%, see Fig. 2. The analyzing power $\hat{a}_{LL}^{\text{PGF}}$ is calculated using the leading-order expressions for the polarized and unpolarized partonic cross-sections and the parton kinematics for each PGF event in the high- p_T Monte Carlo sample. In average, we obtain $\langle \hat{a}_{LL}^{\text{PGF}}/D \rangle = -0.93$, so that the contribution of PGF to the high- p_T asymmetry is $-0.29 \times \Delta G/G$.

The contribution of QCD Compton events to the high- p_T asymmetry is evaluated from a parametrization of the virtual-photon–deuteron asymmetry A_1 based on a fit to the world data [2, 18]. This asymmetry is calculated for each event at the momentum fraction x_q of the quark, known in the simulation. The estimated contribution of the QCD Compton scattering to the high- p_T asymmetry is 0.006.

The parton from a resolved photon interacts either with a quark or a gluon from the nucleon. In the latter case, the process is sensitive to the gluon polarization $\Delta G/G$. The analyzing powers $\hat{a}_{LL}^{ff^\gamma}$ are calculated in pQCD at leading order [19]. The polarizations of the u , d and s quarks in the deuteron $\Delta f/f$ are calculated using the polarized parton distribution functions from Ref. [20] (GRSV2000) and the unpolarized parton distribution functions from Ref. [21] (GRV98, also used as an input for PYTHIA), all at leading order. The polarizations of quarks and gluons in the virtual photon $\Delta f^\gamma/f^\gamma$ are unknown be-

cause the polarized PDFs of the virtual photon have not yet been measured. Nevertheless, theoretical considerations provide a minimum and a maximum value for each Δf^γ , in the so-called minimal and maximal scenarios [22]. As the analyzing powers are positive for all considered channels, the two scenarios correspond to extreme values for the contribution of the resolved-photon processes to the high- p_T asymmetry, $0 + 0.012 \times \Delta G/G$ and $0.002 + 0.078 \times \Delta G/G$, respectively. Here, the term proportional to $\Delta G/G$ comes from the processes involving a gluon from the nucleon.

Our analysis is restricted to leading order, and the systematic error has to take into account next-to-leading-order effects. Their order of magnitude is estimated by repeating the analysis several times with modified Monte Carlo parameters: the renormalization and factorization scales were multiplied and divided by two, and the parton shower mechanism was deactivated. The systematic error is obtained from the difference in the corresponding values for $\Delta G/G$, 0.004 (0.011) in the minimal (maximal) scenario.

Another source of systematic error is the tuning of the PYTHIA parameters. Since our event selection relies on a cut in transverse momentum, the relevant parameters are those which determine the amount of transverse momentum acquired by the outgoing hadrons in the soft parts of the reaction: the intrinsic transverse momentum of the partons in the nucleon and in the resolved photon, and the parameters describing the hadronization. These parameters were scanned independently over a range in which the agreement between the simulation and real data remains reasonable. This results in several values for $\Delta G/G$, all based on the same measured high- p_T asymmetry of Eq. (5). The value of $\Delta G/G$ appears to depend predominantly on the width of the intrinsic-transverse-momentum distribution for the partons in the photon. Varying this parameter between 0.1 GeV/ c and 1 GeV/ c leads to a 30% variation of the fraction of photon–gluon fusion R_{PGF} . Note that the resulting systematic errors are proportional to the high- p_T asymmetry, which implies that a statistical fluctuation of the measured high- p_T asymmetry modifies the systematic errors. This was taken into account by performing the systematic study for $A_{\parallel}/D + \sigma_{\text{stat}}(A_{\parallel}/D)$ and $A_{\parallel}/D - \sigma_{\text{stat}}(A_{\parallel}/D)$ as well, quoting the largest value for the systematic error. Finally, the systematic error on $\Delta G/G$ is 0.018 and 0.052 in the minimal and maximal scenarios, respectively.

5 Result and conclusion

The values for the gluon polarization in the minimal and maximal scenarios are

$$\left(\frac{\Delta G}{G}\right)_{\text{min}} = 0.016 \pm 0.068(\text{stat}) \pm 0.011(\text{exp. syst}) \pm 0.018(\text{MC. syst}), \quad (7)$$

$$\left(\frac{\Delta G}{G}\right)_{\text{max}} = 0.031 \pm 0.089(\text{stat}) \pm 0.014(\text{exp. syst}) \pm 0.052(\text{MC. syst}). \quad (8)$$

This leads to the central value

$$\frac{\Delta G}{G} = 0.024 \pm 0.089(\text{stat}) \pm 0.057(\text{syst}), \quad (9)$$

where the difference between the two scenarios has been included in the systematics, and where all systematics have been added quadratically. Let us recall that the systematic error covers an uncertainty on R_{PGF} of up to 30%. Gluons are probed at an average scale μ^2 and an average momentum fraction of the gluons x_g , which are both obtained from the simulation where the parton kinematics is known. For the scale, we obtain in average

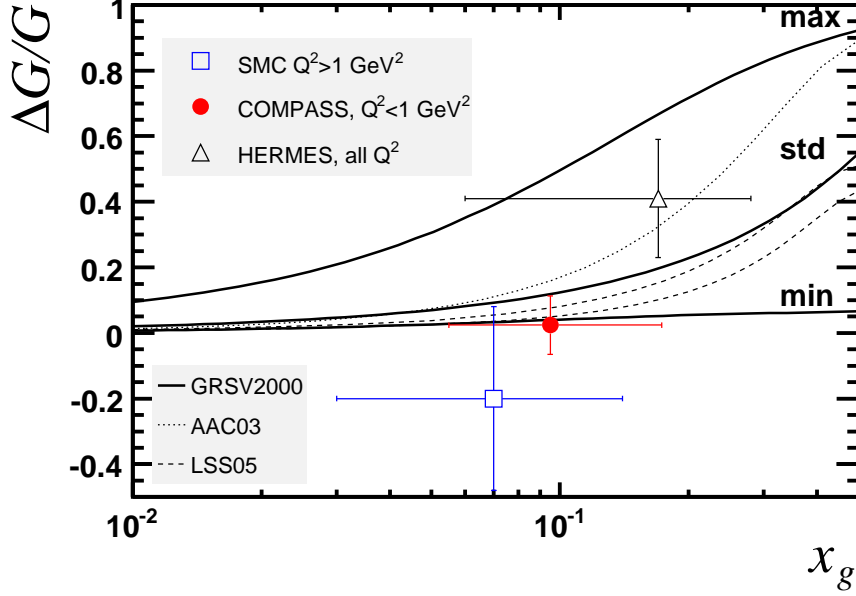


Figure 3: Comparison of the $\Delta G/G$ measurements from COMPASS (present work), SMC [14], and HERMES [23]. The horizontal bar on each point represents the range in x_g . The curves show various parametrizations from NLO fits in the $\overline{\text{MS}}$ scheme at $\mu^2 = 3 \text{ (GeV/c)}^2$: GRSV2000 [20] (3 curves, please see text for details), AAC03 [24], and LSS05 sets 1 and 2 [25].

$\mu^2 \simeq 3 \text{ (GeV/c)}^2$. The distribution of x_g is asymmetric, with a different r.m.s. width on the left and on the right, $x_g = 0.095^{+0.08}_{-0.04}$. For these two quantities, the average was obtained by weighting each event by its sensitivity to the gluon polarization, c.f. Eq. (6).

Our value for the gluon polarization is compared with previous direct measurements from the SMC [14] and HERMES [23] experiments in Fig. 3. The SMC measurement uses high- p_T events at $Q^2 > 1 \text{ (GeV/c)}^2$, where the contribution of the resolved-photon processes is small. The HERMES result was derived from data mostly at low Q^2 , but the contribution of the resolved-photon processes to the asymmetry was neglected. Note that these experimental determinations are based on a leading-order analysis.

Figure 3 also shows three distributions of $\Delta G/G$ as a function of x_g from Ref. [20] (GRSV2000), resulting from QCD fits to the world g_1 data at NLO. They correspond to three hypotheses on the gluon polarization at $\mu^2 = 0.40 \text{ (GeV/c)}^2$: maximal polarization (max), best fit to the data (std), and zero polarization (min). The distributions are then evolved radiatively to $\mu^2 = 3 \text{ (GeV/c)}^2$ where their first moments are 2.5, 0.6 and 0.2, respectively. Our result clearly favors parametrizations with a low gluon polarization.

More recent NLO distributions of $\Delta G/G$ from Ref. [24] (AAC03) and Ref. [25] (LSS05, sets 1 and 2) are displayed as well. Although these curves strongly differ in shape, the values at $x_g = 0.095$ are quite close and all within 1.5σ above our measured value. The first moment ΔG at the scale $\mu^2 = 3 \text{ (GeV/c)}^2$ is equal to 0.8 for AAC03, and to 0.26 (0.39) for LSS05 set 1 (set 2).

When the singlet axial matrix element a_0 was found to be much smaller than the contribution to the nucleon spin expected in the naive quark-parton model, it was suggested that the difference could be accounted for by a large contribution of the gluon

spin [26, 27, 28]. Indeed, in the so-called AB [29] or JET [30] renormalization schemes, the contribution of the quark spins to the nucleon spin becomes $\Delta\Sigma = a_0 + N_f(\alpha_s/2\pi)\Delta G$ where N_f is the number of active flavors. At $Q^2 = 3 \text{ (GeV/c)}^2$, a value of ΔG of about 3 would be required to obtain the expected $\Delta\Sigma$ of the order of 0.6. The small value of $\Delta G/G$ at $x_g = 0.095$ from our measurement cannot by itself rule out the possibility of the first moment ΔG being as large as 3, since the shape of $\Delta G(x_g)$ is poorly known. However, the fact that our point is lower than fitted parameterizations, leading to values of ΔG around or below unity, makes the hypothesis of a large ΔG unlikely.

In summary, we have measured the gluon polarization at $x_g = 0.095$ and $\mu^2 \simeq 3 \text{ (GeV/c)}^2$ and found a result compatible with zero, with a statistical error and a systematic error smaller than 0.1. The gluon polarization was extracted from the longitudinal spin asymmetry obtained for low- Q^2 events in which a pair of high- p_T hadrons is produced. The present analysis, for the first time, takes into account the contribution from the polarized structure of the virtual photon.

Acknowledgments

We gratefully acknowledge the support of the CERN management and staff and the skill and effort of the technicians of our collaborating institutes. Special thanks are due to V. Anosov and V. Pesaro for their technical support during the installation and the running of this experiment. We also thank B. Pire, M. Stratmann, and W. Vogelsang for useful discussions.

References

- [1] EMC, J. Ashman *et al.*, Phys. Lett. B206 (1988) 364; Nucl. Phys. B328 (1989) 1.
- [2] SMC, B. Adeva *et al.*, Phys. Rev. D58 (1998) 112001.
- [3] E155, P. L. Anthony *et al.*, Phys. Lett. B493 (2000) 19, and references therein.
- [4] J. R. Ellis and R. L. Jaffe, Phys. Rev. D9 (1974) 1444.
- [5] A. Watson, Z. Phys. C12 (1982) 123.
- [6] M. Glück and E. Reya, Z. Phys. C39 (1988) 569.
- [7] A. Bravar, D. von Harrach, and A. Kotzinian, Phys. Lett. B421 (1998) 349.
- [8] T. Sjöstrand *et al.*, Computer Physics Commun. 135 (2001) 238.
- [9] G. K. Mallot, Nucl. Instrum. Meth. A518 (2004) 121.
- [10] COMPASS, E. S. Ageev *et al.*, Phys. Lett. B612 (2005) 154.
- [11] J. Ball *et al.*, Nucl. Instrum. Meth. A498 (2003) 101.
- [12] C. Bernet *et al.*, Nucl. Instrum. Meth. A550 (2005) 217.
- [13] C. Friberg and T. Sjöstrand, JHEP 09 (2000) 010.
- [14] SMC, B. Adeva *et al.*, Phys. Rev. D70 (2004) 012002.
- [15] SMC, D. Adams *et al.*, Phys. Rev. D56 (1997) 5330.
- [16] R. Brun *et al.*, CERN Program Library W5013 (1994).
- [17] SMC, B. Adeva *et al.*, Phys. Rev. D60 (1999) 072004.
- [18] E143, K. Abe *et al.*, Phys. Rev. D58 (1998) 112003.
- [19] C. Bourrely, J. Soffer, F. M. Renard, and P. Taxil, Phys. Rept. 177 (1989) 319.
- [20] M. Glück, E. Reya, M. Stratmann, and W. Vogelsang, Phys. Rev. D63 (2001) 094005.
- [21] M. Glück, E. Reya, and A. Vogt, Eur. Phys. J. C5 (1998) 461.
- [22] M. Glück, E. Reya, and C. Sieg, Eur. Phys. J. C20 (2001) 271, (*Note that our definition of the minimal scenario corresponds to a maximum negative polarization of the gluons in the VMD part of the photon*).
- [23] HERMES, A. Airapetian *et al.*, Phys. Rev. Lett. 84 (2000) 2584.

- [24] AAC, M. Hirai, S. Kumano, and N. Saito, Phys. Rev. D69 (2004) 054021.
- [25] E. Leader, A. V. Sidorov, and D. B. Stamenov, JHEP 06 (2005) 033.
- [26] A. V. Efremov and O. V. Teryaev, JINR-E2-88-287.
- [27] G. Altarelli and G. G. Ross, Phys. Lett. B212 (1988) 391.
- [28] R. D. Carlitz, J. C. Collins, and A. H. Mueller, Phys. Lett. B214 (1988) 229.
- [29] R. D. Ball, S. Forte, and G. Ridolfi, Phys. Lett. B378 (1996) 255.
- [30] E. Leader, A. V. Sidorov, and D. B. Stamenov, Phys. Lett. B445 (1998) 232.